Photoresponse of Microwave Transistors to High-Frequency Modulated Lightwave Carrier Signal

Luiz E. M. de Barros, Jr., Arthur Paolella, *Senior Member, IEEE,* Michael Y. Frankel, Murilo A. Romero, Peter R. Herczfeld, *Fellow, IEEE,* and A. Madjar

***Abstract*— Described in this paper are the photoresponse characteristics of microwave transistors, both unipolar [metal–semiconductor FET's (MESFET's) and modulation-doped FET's (MODFET's)] and bipolar [heterojunction bipolar transistors (HBT's)]. Investigation includes time- and frequency-domain measurements. For unipolar devices FET's, the two dominant photodetection mechanisms, photoconductive and photovoltaic, are clearly identified within the same device for the first time. It is shown that even high-speed FET's are limited to a photonic bandwidth of a few megahertz, if photodetection and amplification are to be achieved simultaneously. In contrast, bipolars HBT's can provide optical gain up to the millimeter-wave range. It is shown that their bandwidth to a modulated optical input is closely related to the microwave bandwidth, and that parameters such as base-access resistance and base-emitter capacitance are critical to photoresponse optimization.**

***Index Terms*— Heterojunction bipolar transistors, microwave transistors, optoelectronic devices, photodetectors, phototransistors, transient analysis.**

I. Introduction

THE effects of illumination on microwave transistors and related structures have been the subject of several investigations. The main motivation for this line of research has been to combine photodetection and amplification in a single transistor, potentially simplifying the monolithic optical receiver configuration. Furthermore, the inherent nonlinearity of these transistors renders the possibility for mixing of the modulated optical carrier with a microwave local oscillator (LO), providing for simultaneous up or down-conversion and demodulation of the information signal [1], [2]. In this paper, the gain and bandwidth characteristics of microwave transistors illuminated by time-varying optical signals are considered.

The study of field-effect transistors, namely the metal–semiconductor FET's (MESFET's) [3] and the modulation-doped FET's (MODFET's) [4], as high-speed optical detectors started in the late 1970's. Subsequent to some initial disagreement, it was established that the dominant photodetection mechanism in the MESFET is backgating, caused by the modulation of the channel–substrate junction by the incident illumination, as proposed by Edwards [5]. Madjar *et al*. [6], [7] derived a detailed analytical model to explain this phenomenon, which is supported by extensive experimental characterization [8] and an independent numerical simulation [9].

Photoconductive detectors employing GaAs and InP [4], [10] modulation-doped heterostructures were investigated by a Bell Laboratories research group in the early 1980's. These devices were characterized in the time-domain using high-speed sampling techniques, and yielding encouraging results. Specifically, a 12-ps rise time and a 27-ps full width at half maximum (FWHM) impulse response was obtained. Similar results were achieved using autocorrelation techniques by Umeda *et al*. [11] and Fetterman *et al*. [12]. The detection process was attributed to the direct collection of photoelectrons by the 2-DEG channel.

These time-domain results implying *a priori* large detection bandwidth seem to be in conflict with direct frequency-domain bandwidth measurements, reported by several research groups [13]–[15]. In the frequency-domain, the high-speed response is measured by a microwave network analyzer. When compared to conventional photodiodes, these devices generally display high optical gain at lower frequencies and yield a useful output signal well into the gigahertz range. However, their 3-dB bandwidth is only a few megahertz. This seeming contradiction between the time-domain and frequency-domain measurements can be resolved if one notes that theoretically the photoresponse of MESFET's [6] and MODFET's [16] is comprised of two detection processes, namely a large slow component (photovoltaic) with a low-frequency responsivity which exceeds 10 A/W, and a faster, but much smaller, response (photoconductive) caused by the direct collection of photogenerated electrons.

The slow component, a result of backgating caused by the accumulation of photogenerated holes within the device, has already been explained [7], [8], [16]. However, no direct experimental evidence of the existence of two photodetection mechanisms in the same device has ever been reported.

It is important to point out that there is no correlation between the microwave and photonic bandwidth of the MESFET and the MODFET. For example, the FET's tested are fast microwave devices with f_T in excess of 20 GHz, but their 3-dB cutoff frequency to microwave modulated light is below 20 MHz.

A preferred alternative to the FET's is the bipolar transistor. Earlier research [17] focused on two-terminal devices with

Manuscript received December 12, 1996; revised April 25, 1997. This work was supported in part by the Brazilian Ministry of Education through a Ph.D. fellowship program and the Office of Naval Research.

L. E. M. de Barros, Jr., A. Paolella, M. A. Romero, P. Herczfeld, and A. Madjar are with the Center for Microwave/Lightwave Engineering, Drexel University, Philadelphia, PA 19104 USA.,

M. Frankel is with the Naval Research Laboratory, Washington, DC 20375-5338 USA.

Publisher Item Identifier S 0018-9480(97)06022-5.

bipolar transistor structure, the phototransistors (PT's). These devices were improved in terms of gain with the use of heterostructure PT's (HPT's) [18], [19], but still suffered from speed limitations. In 1991, Chandrasekhar *et al.* [20] have shown that exploiting the third terminal of the HPT with a suitable electrical bias improves both its gain and bandwidth. More recent work on this type of device, namely the heterojunction bipolar transistors (HBT's) [21], [22], demonstrated that the gain-bandwidth product to a modulated optical input is directly related to their microwave properties.

The goals of this paper are:

1) to provide conclusive experimental evidence of the fast and slow detection mechanisms in microwave FETs;
2) to investigate the relation between the electrical bandwidth and the bandwidth to a microwave modulated optical signal in the FET's and HBT's;
3) to discuss the gain-bandwidth characteristics of all three types of microwave transistors, both theoretically and experimentally.

TABLE I
PHORESPONSE LOW-FREQUENCY CURRENT COMPONENTS AND CUTOFF FREQUENCIES FOR FET's

		MESFET	MODFET
Internal photovoltaic	Low frequency response (drain photocurrent)	$g_m m(V_{bar} - V_{ph})\frac{\omega_0}{\omega_C}$ Ref. [7]	$\frac{m(1+\sigma_0)\kappa g_m \tau_p'}{qD}$ Ref.[23]
	cut-off frequency	$\omega_C = \omega_0 + \omega_S$	$\omega_C = 1/2\pi\tau_p'$
Photo-conductive	Low frequency response (drain photocurrent)	$\frac{1}{2}qm\phi_0 A_i e^{-ah_T}(G_n + G_p)\left(\frac{h_{CD}}{L_p}\right)^3 \alpha L_p(1 - 0.5\alpha h_{CD})$ Ref. [7]	$q\phi_0 A_i m[1-\exp(-\alpha W)$ Ref.[23]
	cut-off frequency	$\omega_{high} = (\alpha L_p)^2/\tau_p$	$\omega_{high} = 1/2\pi\tau_{pr}$
Microwave	Low frequency gain	$g_m R_L$	$g_m R_L$
	cut-off frequency	$\omega_C = 1/(R_g C_{gs})$	$\omega_C = 1/(R_g C_{gs})$

II. THEORY

In this section, the photoresponse gain and bandwidth of the three microwave transistors, MESFET, MODFET, and HBT, are discussed. The MESFET and the MODFET are voltage-controlled devices and the HBT is a current-controlled device, a fact that has major implication regarding their optical characteristics. Specifically, the optical illumination, which may be considered an additional control terminal, always generates electron–hole pairs, a primary photocurrent. It will be shown that this primary photocurrent gives rise to fundamentally different photodetection mechanism for the FET's and the HBT, resulting in greatly varying optical responses.

A. Field Effect Transistors: MESFET and MODFET

The photodetection mechanisms of MESFET's and MODFET's are similar in many respects. According to models developed by Paolella *et al.* [6] and Romero *et al.* [16], the intrinsic photoresponse of these devices may be accounted for by two basic transport mechanisms, namely the internal photovoltaic $(I_{\rm pvi})$ and photoconductive $(I_{\rm pc})$ effects. The total photocurrent is the sum of these two currents

$$I_{\rm ph} = I_{\rm pvi} + I_{\rm pc}. \tag{1}$$

The photoconductive effect is the result of increase in conductivity due to photogenerated carriers. In the MESFET, these carriers are generated in the channel while in the MODFET they are created in the depleted buffer region, being drawn to the 2-DEG region by the heterojunction built-in electric field. The photoconductive component of the photoresponse in the MESFET is calculated by solving the continuity equation in the direction of light absorption in the channel and in the MODFET by solving for the drift current due to carriers generated in the depleted buffer layer.

The photocurrent in the photovoltaic effect is a two-step process where a primary photocurrent generates a voltage which controls the flow of thermal carriers. In the MESFET, this voltage is the result of the modulation of the potential barrier between the channel and the substrate [6]. In the MODFET, it is caused by the modulation of the quasi-Fermi level in the channel due to accumulation of holes at the buffer/substrate interface [16]. In both devices, the photovoltaic effect can be represented by an equivalent circuit consisting of a parallel $R_{\rm sub}C$ pair in parallel with a current source $I_{\rm in}$. Physically, C is the channel/substrate barrier capacitance in the case of the MESFET [6], and it is the change in quasi-Fermi level with carrier density [23] for the MODFET, $R_{\rm sub}$ is the substrate resistance and $I_{\rm in}$ is the primary photocurrent generated.

Table I summarizes the low-frequency expressions and cutoff frequencies of the different photoresponse components for these devices. Referring to Table I, κ depends on the layer structure and external geometry of the MODFET, D is the density of states in the 2-DEG channel, τ_p' is the characteristic time constant of the internal photovoltaic effect, $\tau_{\rm pr}$ combines the carriers transit time to reach the 2-DEG channel and the transit in the channel, $V_{\rm bar}$ and $V_{\rm ph}$ are the channel/substrate barrier potential and photovoltage, m is the index of modulation, A_i is the illuminated area, h_T and $h_{\rm CD}$ are the gate depletion region and channel opening due to light, a is the total channel width underneath the gate and R_g is the gate access resistance. The other factors are commonly used parameters.

The expressions reveal the distinct cutoff frequencies for each photodetection mechanism. The photovoltaic effect dominates the spectrum at low frequencies below ω_c. The photovoltaic effect cutoff frequency in the MESFET increases with optical input power and it is governed by the factor ω_0, related to the channel–substrate barrier. The photoconductive cutoff depends only on material parameters and on the specific device structure, therefore, invariant with optical power. Fig. 1 shows the low-frequency components as a function of the incident optical power for the MESFET. Significantly, the ratio of the photovoltaic to photoconductive current is large, in the range of 50–60 dB at an optical input of 1 mW. For low intensities,

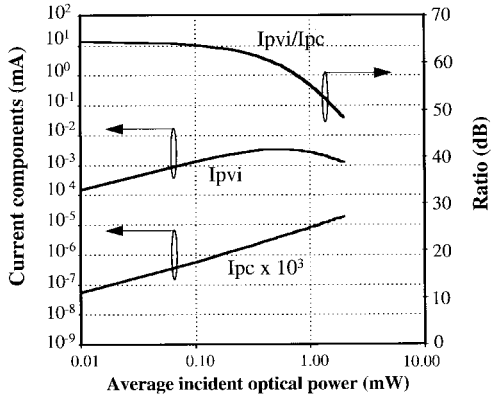

Fig. 1. Low-frequency photocurrent components as a function of incident optical power. Parameters were estimated at $V_{\rm gs} = -0.5$ V, $I_{\rm ds} = 30$ mA.

both components increase with intensity. Beyond a critical point the photovoltaic current decreases with intensity. This is attributed to the fact that the RF gain (proportional to g_m) depends on the dc value of the photovoltage. At very low light levels even a small change in barrier width results in a considerable change in channel opening, increasing the gain with light intensity. At higher intensities, the barrier is greatly reduced and the modulation of its depletion region represents a proportionally smaller fraction of the channel. Therefore, the RF gain will decrease with optical power at moderate to high power levels. These results indicate that for FET devices there exists an optimum illumination level for best gain-bandwidth product.

Consequently, enhancing optical coupling in such devices may not be beneficial in terms of overall photodetection performance. Furthermore, since the photoconductive cutoff frequency is independent of illumination level, the ratio between the bandwidth of the two effects is always a decreasing function of intensity. Similar results are predicted for the MODFET. In this case, estimating τ_p' from the low-frequency response of the measured device (Section III), as in [23], $\tau_p' = 0.16/\mathrm{BW} = 8$ ns, where BW is the bandwidth of the photovoltaic component. Replacing this value in expressions shown in Table I results in a ratio between the photovoltaic and the photoconductive response components of 17–20 dB, due to uncertainty on some of the parameters.

In order to verify the theory, the response in both devices should rolloff at 20 dB/d after $\omega = \omega_C$ and become flat again once the photoconductive effect is dominating over the photovoltaic [24]. The MESFET and MODFET photoconductive responses will start rolling off for frequencies higher than $(\alpha L_p)^2/\tau_p$ and $1/\tau_{\rm pr}$, respectively. It should be stressed at this point that the design considerations for a faster microwave FET, such as reduction of $R_g C_{\rm gs}$ product, do not affect the photoresponse characteristics.

In summary, theoretical considerations for the FET's predict a fast but small photoconductive current and a large but very slow photovoltaic response. The photovoltaic component is slow because it involves a process of converting the primary photocurrent into a photovoltage to control the flow of thermal equilibrium carriers, a process governed by an inherently large *RC* time constant.

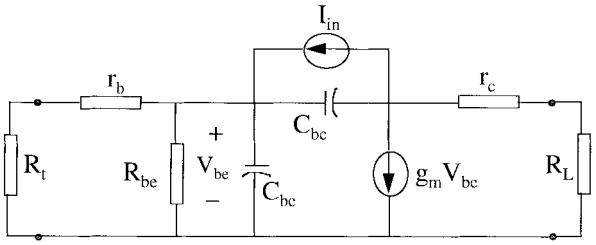

Fig. 2. Common emitter small-signal equivalent circuit for the HBT under illumination.

B. HBT

The illuminated HBT differs from the FET's in the sense that it is a current-controlled current-source device. When illuminated from the top, most of the light is absorbed at the depletion region between base and collector. This region is analogous to a built-in p-i-n diode (p: base, i: collector, and n: subcollector), which provides an electrical input $(I_{\rm in})$ to the base circuit which controls the thermal carriers flowing from emitter to collector [24]. In this case, the current-to-current process allows for a much faster (similar to microwave behavior) detection performance while still maintaining the inherent device current gain.

Under small-signal approximation the common emitter equivalent circuit of the HBT under illumination can be represented as shown in Fig. 2. Although simple, this model is an adequate representation of the HBT under illumination and allows for an analytical solution of the dynamic response. The small-signal approximation implies that the change in $V_{\rm be}$ caused by the modulated light signal is small compared to the thermal potential (26 mV). The termination resistors R_L and R_t are connected to the base and collector of the HBT. The current $I_{\rm in}$ is the primary photocurrent generated in the base–collector depletion region. The frequency response of the circuit is limited by the input circuit impedance combined with the Miller effect component of capacitor C_μ. In an approach similar to Frankel *et al*. [22], where the common-collector configuration was used, it can be shown that the transient time constants of the transimpedance gain $H(s) = V_o(s)/I_{\rm in}(s)$ for the circuit in Fig. 2, are roots of the following polynomial:

$$s^2 + s\frac{[R_{\rm in}(C_{\rm be}+C_{\rm bc}) + (r_c+R_L)C_{\rm bc}(1+g_m R_{\rm in})]}{\tau^2} + \frac{1}{\tau^2} = 0 \tag{2}$$

where $R_{\rm in} = (R_t + r_b)/R_{\rm be}$, $\tau^2 = (R_{\rm in}C_{\rm be}(r_c+R_L)C_{\rm bc})$, and $C_{\rm be}$ is the combined depletion and diffusion base-emitter capacitance.

Under moderate bias currents ($I_c = 1.4$ mA), (2) solves to $\tau_1 = 31$ ps and $\tau_2 = 1.7$ ps where the circuit parameters, extracted from microwave measurements, are: $r_b = 11\ \Omega$, $r_c = 5\ \Omega$, $R_{\rm be} = 650\ \Omega$, $g_m = 52.69 \times 10^{-3}$ S, $C_{\rm be} = 300$ fF and $C_{\rm bc} = 54$ fF. The load resistance and R_t are 50 Ω.

As a result, assuming a Gaussian impulse response, the HBT is expected to have a photoresponse 3-dB bandwidth in excess of 12 GHz. As the bias current is increased, the roots of (2) lead to larger transient time constants and consequently a slower photoresponse. This behavior is expected since the

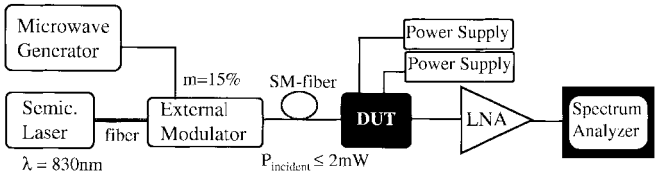

Fig. 3. Experimental setup for frequency-domain measurements of the photoresponse spectrum of microwave transistors.

total base-emitter capacitance will increase with current flow at moderate biases [25]. Under small signals, the low-frequency gain of the photoresponse is proportional to the transconductance which increases with collector current. Therefore, a tradeoff between gain and bandwidth is apparent for the HBT.

In order to fully characterize the photo-dynamic processes in these microwave transistors and clarify the discordance in the literature, both frequency and time-domain experiments were performed in all devices.

III. Frequency-Domain Characterization

A 20-mW semiconductor laser operating at 830 nm coupled to a single-mode fiber was used as the light source in Fig. 3. The microwave signal was superimposed on the optical carrier by means of an electro-optic modulator (8-GHz bandwidth). The modulation index was 15% for all experiments and illumination was perpendicular to the electrode surface of the devices. The device output current was amplified and displayed in a spectrum analyzer. A low-noise amplifier (LNA) was used, specifically in the case of the photoconductive component of FET's ($f \geq 300$ MHz).

The AlGaAs/GaAs microwave MODFET's investigated had a gate length of 0.25 μm, $f_T = 58$ GHz at $I_{\rm ds} = 16$ mA and areas between gate and drain electrodes of 2×10 μm^2. For the first time, two distinct cutoff frequencies are clearly identified in the photoresponse spectrum shown in Fig. 4. The first cutoff (around 20 MHz) is due to the internal photovoltaic effect. The second cutoff $\sim$ 1.0 GHz is attributed to the photoconductive effect. Furthermore, the ratio between these two photoresponse components (16 dB) is in good agreement with the predicted value (17 dB). It should also be noted that the rise of the response at very low frequencies is due to the response of the biasing circuit of the MODFET. The gain-bandwidth product is a monotonically decaying function of the incident optical power, as reported elsewhere [16].

The GaAs MESFET had the following characteristics: $R_{\rm sub} = 1 \times 10^6$-$\Omega$ channel thickness under the gate of 0.25 μm doped at 4.45×10^{17} cm^{-3}, $f_s = 20$ GHz at $I_{\rm ds} = 30$ mA. The analytical expressions in Table I and the results in Fig. 1 demonstrate that the ratio between the two photocurrent components can be as high as 55 dB, for a typical microwave transistor biased at open-gate condition ($V_{\rm gs} = -0.5$, $I_{\rm ds} = 30$ mA) and illuminated by moderate optical powers ranging from 0.5 to 1.5 mW. Furthermore, the gain-bandwidth product (shown in Fig. 5) is dependent on the optical input power. Both simulated and theoretical results determined 0.6-mW average incident power as the optimum illumination level for the best gain-bandwidth result in this particular device. In this

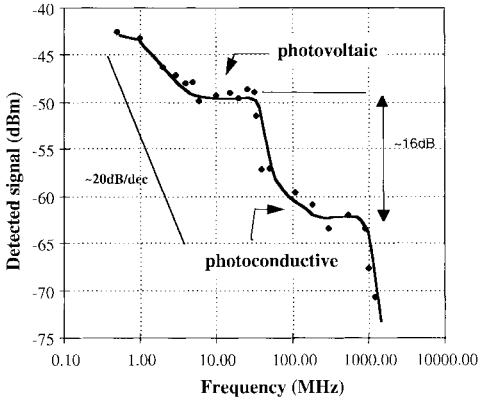

Fig. 4. Photoresponse spectrum of the MODFET at $V_{\rm gs} = -0.2$ V, $I_{\rm ds} = 16$ mA.

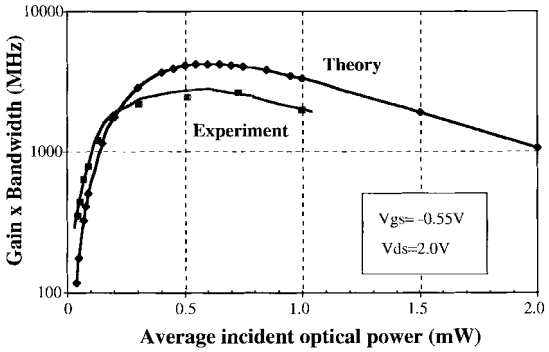

Fig. 5. MESFET gain-bandwidth product as a function of the average incident optical power. A commercial p-i-n diode (0.4 A/W) with signal output of -45 dBm at 1 mW of optical input and modulation index of 15% is used as reference for gain. The 3-dB bandwidth is used when calculating the gain-band product.

case, the gain is defined with respect to a high-speed p-i-n diode (0.4 A/W) which produces an output signal power of -45 dBm at 1-mW optical power with modulation index of 15%. Typically, 2.5-GHz peak gain-bandwidth product can be achieved at the optimum illumination level. Overall, very good agreement is observed between theory and experiment.

The normalized spectrum of the MESFET photoresponse in relation to the above-mentioned p-i-n diode (0 dB line), is shown in Fig. 6. The photovoltaic bandwidth is 9 MHz, when biased at $V_{\rm gs} = -0.5$ V, and presents a 20-dB/d rolloff, as expected. However, at this bias level the difference between the photovoltaic and photoconductive response is estimated to be 55 dB, which effectively precludes the direct observation of the photoconductive current. In other words, for this case, $(\alpha L_p)^2/\tau_p < 9$ [7], which means that the photoconductive effect would reach cutoff before becoming the dominant component in the photoresponse. However, by driving the MESFET close to pinchoff, $V_{\rm gs} = -1.1$ V, the transconductance is greatly reduced, minimizing the photovoltaic effect and, thereby, allowing for the observation of the photoconductive contribution, as clearly illustrated in curve b of Fig. 6. The photoconductive cutoff is 3.5 GHz. Curve c of Fig. 6 is the measured MESFET microwave (electric) response, actual $S21$, with 3-dB bandwidth of 7 GHz.

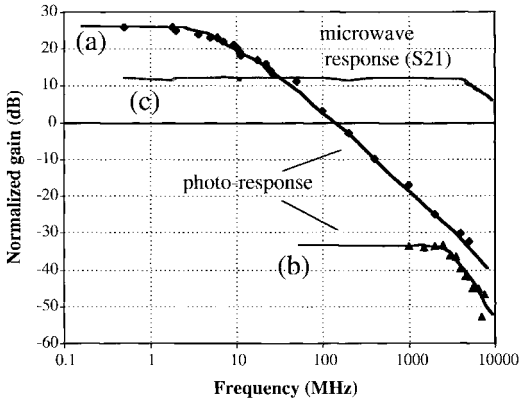

Fig. 6. Curves a and b are the MESFET normalized photoresponse spectrum at $V_{\rm gs} = -0.5$ V, $I_{\rm ds} = 30$ mA, and $V_{\rm gs} = -1.1$ V, $I_{\rm ds} = 3$ mA, respectively. The gain is normalized with respect to the reference p-i-n diode (0-dB line). The average incident optical power is 1 mW. Curve c is the microwave (electric) response $S21$ of the MESFET at $V_{\rm gs} = -0.5$ V, $I_{\rm ds} = 17$ mA. The bias points in a and c are the same. The difference in drain current is due to the optical input.

These results reveal the small correlation between the photonic- and electronic-response speeds. Specifically, the photovoltaic bandwidth is three orders of magnitude smaller than the electrical bandwidth. Similar results are observed for the MODFET, which presented microwave gain-bandwidth product (f_T) of 58 GHz at 16 mA.

The n-p-n self-aligned HBT structure consisted of 5000 Å GaAs n-doped at 2×10^{18} cm^{-3} sub-collector, 5000-Å GaAs intrinsic collector, 800 Å GaAs p-doped at 2×10^{19} cm^{-3} base, and 400 Å AlGaAs n-doped at 5×10^{17} cm^{-3} emitter. The emitter-cap layer width is 3000 Å and doped at 2×10^{18} cm^{-3}. The illuminated area is 1.5×10 μm^2. The HBT photoresponse follows its microwave characteristics. In this case, the bandwidth-limited (8-GHz) frequency measurement setup described earlier is unable to characterize the complete photoresponse spectrum of the HBT. Therefore, to investigate its high-frequency response, a time-domain measurement setup is used.

IV. Time-Domain Characterization

The MODFET and HBT were characterized in the time domain using a mode-locked Ti:Saphire laser operating at 814 nm. The generated pulses were 120-fs wide with 100-MHz repetition rate and maximum average optical power of 4.9 mW. The devices were illuminated from the top and the incident-beam spot size was adjusted so that coupling efficiencies were the same as in the frequency-domain experiment. The photoresponse measurements were performed with a 50-GHz sampling oscilloscope using 60-GHz coplanar waveguide (CPW) probes, presenting an apparent 50-Ω impedance to the devices under test.

The normalized impulse response, with respect to peak value, of the MODFET with two distinct bias conditions, open channel ($V_{\rm gs} = -0.2$ V, $I_{\rm ds} = 16$ mA) and pinchoff ($V_{\rm gs} = -1.0$ V, $I_{\rm ds} = 0.08$ mA), is shown in Fig. 7(a). At $V_{\rm gs} = -0.2$ V the MODFET has maximum transconductance, and at $V_{\rm gs} = -1.0$ V the dark current in the channel is negligible. Under open-channel condition the impulse response

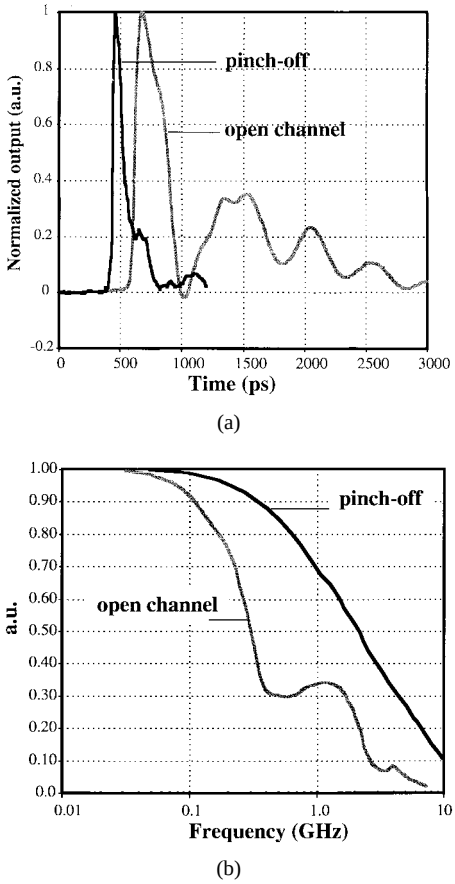

Fig. 7. (a) MODFET normalized drain current response to optical impulse excitation for different bias conditions: open channel, $V_{\rm gs} = -0.2$, $V_{\rm ds} = 2$ V and pinchoff, $V_{\rm gs} = -1.0$ V, $V_{\rm ds} = 2.0$ V. (b) Amplitude Fourier spectrum of the impulse response.

is clearly comprised of two time constants: a short one related to the fast rise time (photoconductive effect) and a long one which is identified by the slow decaying oscillations. The multiple peaks in the trailing edge of the pulse are caused by the repetition rate of the laser which is faster than the photovoltaic response (long time constant). Under pinchoff conditions, elimination of the slow photovoltaic response produces an impulse response with a faster fall time and an overall larger bandwidth, at the expense of gain. Fig. 7(b) depicts the normalized Fourier amplitude spectrum of the impulse responses of Fig. 7(a). The flat region in the open-channel curve marks where the photoconductive effect starts to dominate the photoresponse, confirming the microwave-domain results shown in Fig. 4. With the device under pinchoff conditions, the 3-dB bandwidth of 1 GHz for the photoconductive effect is clearly identified in the Fourier spectrum. These results using time- and frequency-domain measurements, for the first time, conclusively validate the existence of the two time constants, as predicted by the theory.

The HBT impulse response in a common-emitter configuration is analyzed in Fig. 8(a) and (b) as a function of biasing current. In Fig. 8(a), FWHM of 20 ps is obtained for a collector current of 10 μA and 31 ps for a current of 1.4 mA. The Fourier amplitude spectrum of the two curves, at 1.4 mA and 10 μA, with bandwidths of 4 and 10 GHz, respectively, is

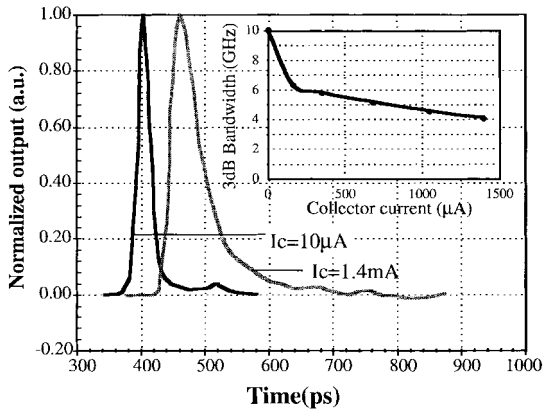

(a)

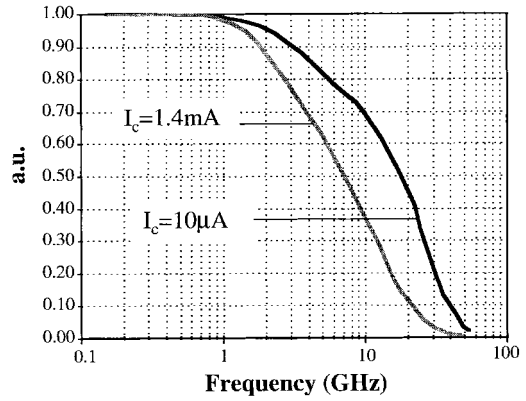

(b)

Fig. 8. (a) HBT collector current response to optical impulse excitation at $I_c = 10\ \mu$A and $I_c = 1.4$ mA. Inset shows 3-dB bandwidth as a function of collector current. (b) Amplitude Fourier spectrum of the impulse response.

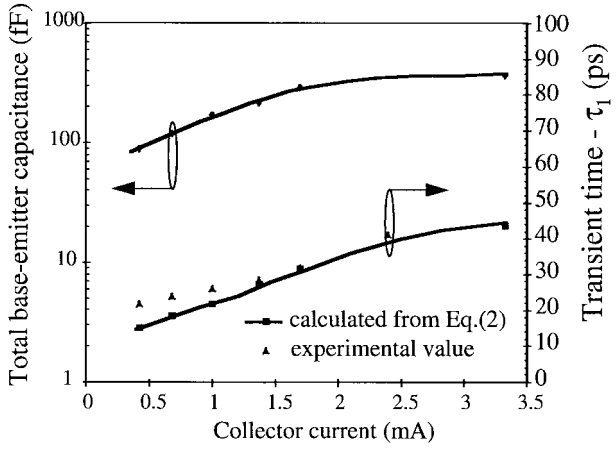

Fig. 9. Total base-emitter capacitance and calculated and experimental transient time as a function of the collector current.

shown in Fig. 8(b). The insert shows that the photoresponse bandwidth of the HBT in common-emitter configuration is a decreasing function of the dc-collector current.

As the collector current is increased, the fall time is extended as a result of increased total base-emitter capacitance, as predicted by (2). The total capacitance $C_{\rm be}$ extracted from microwave measurements and the associated transient time as a function of the collector current are shown in Fig. 9. The divergence between measured and expected transient duration, especially at lower currents, is attributed to the influence of two-dimensional (2-D) effects such as the base-spreading resistance and the external base–collector capacitance, not represented in the model of Fig. 2. However, a good overall agreement is observed. Significantly, these results reveal that the gain and bandwidth of the HBT for microwave or optical inputs are correlated and nearly identical. In this case, the HBT presented f_T of 28 GHz at 1.4 mA. This implies that a faster microwave HBT (small $r_bC_{\rm be}$ and low-spreading resistance) invariably leads to a faster optical detector.

V. Conclusion

The photoresponse characteristics of microwave transistors such as MESFET's, MODFET's and HBT's were theoretically and experimentally investigated. The confusion regarding the photoresponse speed of microwave MESFET's and MODFET's was resolved by the first complete characterization of the two dominant photomechanisms in these devices. By using frequency- and time-domain techniques, the high-gain slow photovoltaic effect, and the small-gain, but fast, photoconductive mechanism were clearly identified in the same device. Although having microwave (electronic) gain-bandwidth product in excess of 50 GHz, these devices are limited to a few tens of megahertz for photonic applications (simultaneous detection and amplification). It was also shown that in the case of MESFET's the gain-bandwidth product may be maximized by the proper input optical power level. Furthermore, the optimization rules used for microwave FET's do not necessarily apply for photonic applications.

The HBT in the common emitter configuration can maintain significant optical gain (proportional to g_m) well into the gigahertz range. The base bias-current provides a means of trading gain for bandwidth where the increase in current increases the gain and reduces the 3 dB-bandwidth. In these devices, the photonic bandwidth is closely related to the electronic (microwave) bandwidth. Since the new generation of microwave HBT's can have gain-bandwidth products in excess of several hundreds of gigahertz, there is enormous potential to fabricate an optical detector with similar gain-bandwidth products as well. OEIC receivers with HBT photodetectors will be able to replace presently used device combinations in many applications involving high-speed fiber-optic links.

Acknowledgment

The authors would like to thank E. Niehenke and B. Fennel from Northrop Grumman, Baltimore, MD, for their help in the microwave characterization of the devices and Dr. I. Bahl from ITT, Roanoke, VA, for the donation of the MESFET's.

References

[1] C. Rauscher and K. J. Williams, "Heterodyne reception of millimeter-wave modulated optical signals with an InP based transistor," *IEEE Trans. Microwave Theory Tech.*, vol. 42, pp. 2027–2034, Nov. 1994.

[2] E. Suematsu and N. Imai, "A fiber optic/millimeter-wave radio transmission link using HBT as direct photodetector and an optoelectronic up-converter," *IEEE Trans. Microwave Theory Tech.*, vol. 44, pp. 133–143, Jan. 1996.

[3] C. Baack, G. Elze, and G. Walf, "GaAs MESFET: A high-speed optical detector," *Electron. Lett.*, vol. 13, no. 7, p. 193, July 1977.
[4] C. Y. Chen, A. Y. Cho, C. G. Bethea, and P. A. Garbinski, "Bias-free selectively doped AlGaAs-GaAs picosecond photodetectors," *Appl. Phys. Lett.*, vol. 41, no. 3, pp. 282–282, Aug. 1982.
[5] W. D. Edwards, "Two and three terminal gallium arsenide FET optical detectors," *IEEE Electron Device Lett.*, vol. EDL-1, pp. 149–150, Aug. 1980.
[6] A. Madjar, A. Paolella, and P. R. Herczfeld, "Analytical model for optically generated currents in GaAs MESFET's," *IEEE Trans. Microwave Theory Tech.*, vol. 40, pp. 1681–1691, Aug. 1992.
[7] A. Madjar, A. Paolella, and P. R. Herczfeld, "Modeling the GaAs MESFET's response to modulated light at radio and microwave frequencies," *IEEE Trans. Microwave Theory Tech.*, vol. 42, pp. 1122–1130, July 1994.
[8] A. Paolella, "The photoresponse of the GaAs metal semiconductor field effect transistor," Ph.D. dissertation, ECE Dept., Drexel University, Philadelphia, PA, 1992.
[9] S. H. Lo and C. P. Lee, "Numerical analysis of the photoeffects in GaAs MESFET's," *IEEE Trans. Electron Devices*, vol. 39, pp. 1564–1570, July 1992.
[10] C. Y. Chen, Y. M. Pang, K. Alavi, A. Y. Cho, and P. A. Garbinski, "Interdigitated AlInAs/GaInAs photoconductive detectors," *Appl. Phys. Lett.*, vol. 44, no. 1, pp. 99–101, Jan. 1984.
[11] T. Umeda, Y. Cho, and A. Shibatomi, "Picosecond HEMT photodetector," *Jpn. J. Appl. Phys.*, vol. 25, no. 10, pp. L801–L803, Oct. 1986.
[12] M. Z. Martin, F. K. Oshita, M. Matloubian, H. R. Fetterman, L. Shaw, and K. L. Tan, "High-speed optical response of pseudomorphic InGaAs high electron mobility transistor," *IEEE Photon. Technol. Lett.*, vol. 4, pp. 1012–1014, Sept. 1992.
[13] P. C. Claspy and K. B. Bhasin, "Microwave response of a HEMT photoconductive detector," *Microwave Opt. Technol. Lett.*, vol. 2, no. 1, pp. 1–3, Jan. 1989.
[14] S. Banba, E. Suematsu, and H. Ogawa, "Fundamental properties of HEMT photodetectors for use in fiber optic links," presented at the *Proc. 23rd. European Microwave Conf.*, Madrid, Spain, Sept. 1993.
[15] A. Bangert, J. Rosenzweig, M. Ludwig, W. Bronner, P. Hofmann, and K. Kholer, "Optical response of a pseudomorfic HFET up to 10 GHz," in *Proc. IEEE/MTT-S*, vol. 3, San Diego, CA, May 1994, pp. 1395–1398.
[16] M. A. Romero, M. A. G. Martinez, and P. R. Herczfeld, "An analytical model for the photedetection mechanisms in high-electron mobility transistors," *IEEE Trans. Microwave Theory Tech.*, vol. 44, pp. 2279–2287, Dec. 1996.
[17] P. Gary and J. Linvill, "Modeling of steady-state optical phenomena in transistors and diodes," *IEEE Trans. Electron Devices*, vol. ED-15, pp. 267–274, May 1968.
[18] T. Morizzumi and K. Takahashi, "Theoretical analysis of heterostructure phototransistors," *IEEE Trans. Electron Devices*, vol. ED-19, pp. 152–159, Feb. 1972.
[19] J. C. Campbell, "Phototransistors for lightwave communications," *Semiconduct. Semimetals*, pt. D, vol. 22, pp. 389–447, 1985.
[20] S. Chandrasekhar, M. K. Hoppe, A. G. Dentai, C. H. Joyner, and G. J. Qua, "Demonstration of enhanced performance of an InP/InGaAs heterojunction phototransistor with a base terminal," *IEEE Trans. Electron Device Lett.*, vol. 12, pp. 550–552, Oct. 1991.
[21] H. Fukano, Y. Takahashi, and M. Fugimoto, "High-speed InP-InGaAs heterojunction phototransistors employing a nonalloyed electrode metal as a reflector," *IEEE J. Quantum Electron.*, vol. 30, pp. 2889–2895, Dec. 1994.
[22] M. Frankel, T. Carruthers, and C. Kyono, "Analysis of ultrafast photocarrier transport in AlInAs-GaInAs heterojunction bipolar transistors," *IEEE J. Quantum Electron.*, vol. 31, pp. 278–285, Feb. 1995.
[23] M. A. Romero, "Modulation doped field effect photodetectors," Ph.D. dissertation, ECE Dept., Drexel University, Philadelphia, PA, 1995.
[24] L. E. M. de Barros, A. Paolella, P. Herczfeld, and A. A. A. de Salles, "The optical performance of microwave transistors," in *IEEE MTT Symp. Proc.*, vol. 3, San Francisco, CA, June 1996, pp. 1445–1448.
[25] S. Tiwari, *Compound Semiconductor Device Physics*. New York: Academic, 1992.

Luiz E. M. de Barros, Jr. was born in Itaperuna, Rio de Janeiro, Brazil, in 1966. He received the B.Sc. degree in electrical engineering from Pontifical Catholic University of Rio de Janeiro, Rio de Janeiro, Brazil, in 1989, the M.Sc. degree in electrical engineering from State University of Campinas, Campinas, São Paolo, Brazil, in 1992, and is currently pursuing the Ph.D. degree at Drexel University, Philadelphia, PA.

His research interests are semiconductor device physics, optoelectronic integrated circuits, high-speed microwave-lightwave interfaces, infra-red sensors, and bio-photonics.

Arthur Paolella (S'90–M'92–SM'92), photograph and biography not available at the time of publication.

Michael Y. Frankel was born in St. Petersburg, Russia, in 1964. He received the B.S. degree (magna cum laude) from the University of Maryland at College Park, in 1986, the M.S. degree from the University of Rochester, Rochester, NY, in 1988, and the Ph.D. degree from the University of Michigan at Ann Arbor, in 1991, all in electrical engineering.

He is currently with the Optical Sciences Division, Naval Research Laboratory, Washington, DC. He has authored over 50 publications and conference presentations and holds several patents. He is actively pursuing novel photonic beamforming techniques for phase-array antennas. He is also involved in developing techniques and components for fiber-optic links. His other interests are in ultrafast optoelectronic studies and modeling of semiconductor materials, high-speed transmission lines, photodetectors, and transistors.

Murilo A. Romero was born in Rio de Janeiro, Brazil, in 1995. He received the B.Sc. and M.Sc. degrees, both in electrical engineering, from Pontifical Catholic University of Rio de Janeiro, Rio de Janeiro, Brazil, in 1988 and 1991, respectively, and the Ph.D. degree from Drexel University, Philadelphia, PA, in 1995.

Since 1995, he has been an Assistant Professor at University of São Paulo, São Carlos, Brazil. His current research interests are optical fiber sensors, nonlinear photonics and the modeling and simulation of optoelectronic semiconductor devices and circuits.

Peter R. Herczfeld (S'66–M'67–SM'89–F'91) was born in Budapest, Hungary, in 1935. He received the B.Sc. degree in physics from Colorado State University, Fort Collins, in 1961, and the M.Sc. degree in physics and Ph.D. degree in electrical engineering from the University of Minnesota, Minneapolis, in 1963 and 1967, respectively.

Since 1967, he has been on the faculty of Drexel University, Philadelphia, PA, where he is both a Professor of electrical and computer engineering, and Director of the Center for Microwave–Lightwave Engineering. He has published over 300 papers in solid-state electronics, microwaves, photonics, solar energy, and biomedical engineering, and has served as Project Director for over 70 projects.

Dr. Herczfeld is a member of APS, SPIE, and ISEC, and is recipient of several research and publication awards, including the Microwave Prize in 1986 and 1994.

A. Madjar, photograph and biography not available at the time of publication.